



Full paper/Mémoire

# Synthesis and characterization of polymer/microporous molecular sieve nanocomposite as a shape-selective basic catalyst

Roozbeh Javad Kalbasi\*, Elham Izadi

Department of Chemistry, Shahreza Branch, Islamic Azad University, 311-86145, Shahreza, Isfahan, Iran

## ARTICLE INFO

## Article history:

Received 22 February 2011

Accepted after revision 3 May 2011

Available online 24 June 2011

## Keywords:

Heterogeneous catalysis  
Organic–inorganic hybrids  
Microporous materials  
Polymers

## ABSTRACT

This paper reports the preparation and characterization of poly(4-vinylpyridine)/AlPO<sub>4</sub>-11 nanocomposite and its application in Knoevenagel condensation as a novel basic catalyst. The catalyst was characterized by XRD, XRF, FT-IR, TGA, BET, SEM, and back titration using NaOH and TPD techniques. Several AlPO<sub>4</sub>-11 with different Al/P ratios were prepared, and the effect of the Al/P ratio on the surface properties and acidity of the support were studied. The use of AlPO<sub>4</sub>-11 as a new supporting material for the Poly(4-vinylpyridine) was tested for the Knoevenagel condensation. Excellent yields at room temperature in aqueous and solvent-free conditions were obtained by this nanocomposite. Accordingly, the catalyst showed shape selectivity in the Knoevenagel reaction. It was observed that the activity of the catalyst just decreased to 90% after five regeneration processes were performed.

© 2011 Académie des sciences. Published by Elsevier Masson SAS. All rights reserved.

## 1. Introduction

Recently, heterogenization of homogeneous catalysts has become an important strategy for the preparation of supported catalysts, which have the combined advantages of homogeneous and heterogeneous catalysts such as high selectivity, reusability and ease of separation [1]. In heterogeneous catalysts, various support matrices such as organic polymers and inorganic silica, especially porous inorganic materials with high surface areas, have been employed [2,3]. Nowadays, design and preparation of organic–inorganic hybrid catalysts based on molecular sieves which are achieved by functionalizing the porous system [4,5], are of great interest.

Aluminophosphate molecular sieves (AlPO<sub>4</sub>-*n*) are a family of microporous crystalline materials developed in 1982 by Wilson et al. [6]. Amorphous aluminum phosphate is built of tetrahedral units of AlO<sub>4</sub> and PO<sub>4</sub>, and is structurally similar to silica. They have many structures including neutral zeolite-like open-frameworks, and a

range of anionic open-frameworks with 3-dimensional (3-D) framework, 2-D layer, 1-D chain, and 0-D cluster structures [7,8]. In recent years, aluminum phosphate is receiving considerable attention as a support for a variety of catalytic reactions [9]. High surface area and controllable pore size distributions are the main reasons for using amorphous AlPO<sub>4</sub> as support. It is anticipated that the AlPOs molecular sieve will have only weak catalytic and sorption properties due to inherent lack of active sites, which are necessary for catalysis. In general, the basicity in calcined AlPO<sub>4</sub> molecular sieve is achieved by functionalizing its microporous, and surfaced with compounds containing organic bases or basic polymers.

Micropore crystalline AlPO<sub>4</sub>-11 (AEL framework topology) is a member of the aluminophosphate molecular sieves family, which has a unique three-dimensional structure with orthorhombic symmetry, *a* = 13.534 Å, *b* = 18.482 Å, *c* = 8.370 Å, high thermal and hydrothermal stability [10,11]. AlPO<sub>4</sub>-11 molecular sieve has 10-membered ring channels with elliptical pore apertures of 0.63 × 0.39 nm [12,13].

Organic–inorganic polymer hybrid materials have received a great deal of attention in recent years [14,15]. In the hybrid materials, the inorganic and organic phases

\* Corresponding author.

E-mail address: rkalbasi@iaush.ac.ir (R.J. Kalbasi).

are combined by the interactions including hydrogen bonds and chemical covalent bonds. The hybrids have organic and inorganic elements that are mixed in a molecular level, and the intimate mixing provides various properties that are different from those of traditional composites. The stability, low density, flexibility and low manufacturing cost make these hybrid polymers amenable for industrial applications [16].

Recently, scientists have synthesized a hybrid polymer/aluminophosphate nanocomposite with layered aluminophosphates and different Al/P ratios [17,18]. These materials are mostly used as gas or liquid separators, not catalysts. There are many reports on the catalytic activity of Lewis acid ion-exchanged  $\text{AlPO}_4$ -11 for many reactions of industrial importance [19]. However, there is no literature report on synthesis, characterization and application of polymer/ $\text{AlPO}_4$  nanocomposite as heterogeneous basic catalyst.

In our previous studies, Knoevenagel condensation over heterogeneous basic catalyst using mesoporous materials such as SBA-15 was carried out [14,20]. In the present work, we wish to introduce a novel hybrid material, poly(4-vinylpyridine) supported over micropore  $\text{AlPO}_4$ -11 by in situ polymerization of 4-vinyl pyridine (4VP) in the presence of  $\text{AlPO}_4$ -11 (Scheme 1). The main goals of this catalytic synthesis were to prepare a shape selective basic catalyst and to compare this novel micropore nanocomposite with other mesoporous composites prepared in the previous studies [14,20].

The basic catalytic activity and the shape-selectivity of this organic-inorganic hybrid were tested for Knoevenagel condensation in water and solvent-free condition.

## 2. Experimental

### 2.1. Materials

All organic reagents were supplied from Sigma-Aldrich, Merck, and were used as received without further purification.

### 2.2. Characterization

The morphological and structural characteristics of the  $\text{AlPO}_4$ -11 supports and poly(4-vinylpyridine)/ $\text{AlPO}_4$  nanocomposites were measured by XRD (Bruker D8ADVANCE,  $\text{Cu K}_\alpha$  radiation), XRF (Bruker S<sub>4</sub> Pioneer), FT-IR spectroscopy

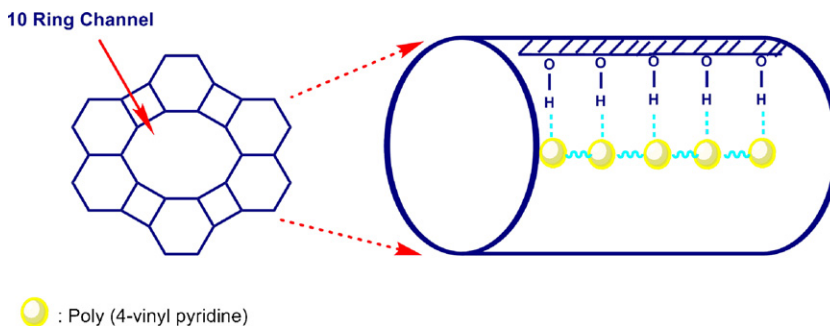
(Nicolet 400D in KBr matrix in the range of 4000–400  $\text{cm}^{-1}$ ), SEM (Philips XL20) and thermal analyzer TGA (Setaram Labsys TG [STA] in temperatures 30–700 °C and heating rate of 10 °C/min in  $\text{N}_2$  atmosphere), respectively. The specific surface area was calculated using the Brunauer–Emmett–Teller (BET) method.  $\text{N}_2$ -BET surface areas and pore volumes were determined on a series BEL SORP 18 apparatus, at 77 K. The nitrogen adsorption isotherms of the  $\text{AlPO}_4$ -11 (Al/P = 1.2) and P4VP/ $\text{AlPO}_4$ -11 (Al/P = 1.2) were obtained at 120 °C. The pore size distributions were obtained from the adsorption and desorption branch of the nitrogen isotherms by the Barrett–Joyner–Halenda (BJH) method. Mesopore surface areas and micropore volumes were determined by the *t*-plot method. The temperature programmed desorption (TPD) of  $\text{NH}_3$  was made using a TPD/TPR 2900 (Mirmirics Company). The products were characterized by  $^1\text{H}$  and  $^{13}\text{C}$  NMR spectra (Bruker DRX-500 Avance spectrometer at 500.13 and 125.47 MHz, respectively). Melting points were measured on an electrothermal 9100 apparatus and reported without correction. All the products were known compounds and they were characterized by FT-IR,  $^1\text{H}$  NMR and  $^{13}\text{C}$  NMR. All melting points were compared satisfactorily with those reported in the literature.

### 2.3. Catalyst synthesis

Several  $\text{AlPO}_4$ -11 with different gel compositions have been synthesized (Table 1).

#### 2.3.1. Synthesis of $\text{AlPO}_4$ -11

$\text{AlPO}_4$ -11 was prepared using di-*n*-propylamine ( $n\text{-Pr}_2\text{NH}$ ) as the template [10,11]. The control of the synthesis condition especially Al/P ratio is a key factor for the formation of an efficient support. We believe that the Al/P ratio has a direct effect on acidic-basic property and activity of the  $\text{AlPO}_4$  as the support. The catalysts with varied Al/P atomic ratios were prepared under hydrothermal condition for choosing the best support for attachment of poly(4-vinylpyridine) on the surface of  $\text{AlPO}_4$ -11 (Table 1). The general procedure was as follows: aluminum triisopropoxide ( $\text{Al}[\text{iPrO}]_3$ ) was dissolved in distilled water and this mixture was stirred for 75 minutes. The phosphoric acid (85%  $\text{H}_3\text{PO}_4$ ) was added drop-wise and the mixture was stirred for 75 minutes. After that,  $n\text{-Pr}_2\text{NH}$  was added drop-wise into the solution and the mixture was stirred for 75 minutes to form a homogeneous gel. The



Scheme 1. Polymerization of 4-vinyl pyridine in the presence of  $\text{AlPO}_4$ -11.

**Table 1**  
Experimental conditions and results for the crystallization of AlPO<sub>4</sub>-11 molecular sieve using conventional heating.

Entry	Molar gel composition	Template	Al/P ratio	T (°C)	Time (h)	Starting PH	Product phase
1	1.1Al <sub>2</sub> O <sub>3</sub> :1.3P <sub>2</sub> O <sub>5</sub> :2DPA:50H <sub>2</sub> O	Di-n-propylamine	1.1:1.3	160	48	5.5	AlPO <sub>4</sub> -11
2	1.1Al <sub>2</sub> O <sub>3</sub> :1.73P <sub>2</sub> O <sub>5</sub> :1.6DPA:70H <sub>2</sub> O	Di-n-propylamine	1.1:1.73	200	96	5.5	AlPO <sub>4</sub> -11
3	1.1Al <sub>2</sub> O <sub>3</sub> :0.9P <sub>2</sub> O <sub>5</sub> :1.6DPA:70H <sub>2</sub> O	Di-n-propylamine	1.1:0.9	200	96	5.5	AlPO <sub>4</sub> -11
4	1Al <sub>2</sub> O <sub>3</sub> :2.5P <sub>2</sub> O <sub>5</sub> :1.6DPA:70H <sub>2</sub> O	Di-n-propylamine	1.0:2.5	200	96	5.5	AlPO <sub>4</sub> -11
5	1Al(i-PrO) <sub>3</sub> :1.8H <sub>3</sub> PO <sub>4</sub> :1.5EA:78H <sub>2</sub> O	Ethylamine	1.0:1.8	180	96	5.7	AlPO <sub>4</sub> -11 (90%)

DPA: di-n-propylamine; EA: ethylamine.

pH values of the prepared gels was adjusted to 5.5 by drop-wise addition of mixture of HCl and H<sub>2</sub>O with molar ratio of 1:1, and this gel was transferred into a Teflon-lined stainless steel autoclave and heated under autogenous pressure at 200 °C for 96 hours. The nanocrystalline products were obtained after they were filtered, washed with distilled water and dried at 80 °C for 10 hours. The sample was calcined under airflow at 405 °C for 5 hours to remove the organic template material.

The best molar gel composition that is chosen for synthesis of the AlPO<sub>4</sub>-11 as an efficient support is Al/P = 1.2 (Table 1, entry 3).

### 2.3.2. Preparation of poly(4-vinylpyridine)/AlPO<sub>4</sub>-11 nanocomposite

Various nanocomposites with AlPO<sub>4</sub>-11 containing different Al/P molar ratios were synthesized and tested for Knoevenagel condensation. The general procedure was as follows: poly(4-vinylpyridine)/AlPO<sub>4</sub>-11 (P4VP/AlPO<sub>4</sub>-11) was synthesized as follows (Scheme 2): AlPO<sub>4</sub> (0.5 g) and 4-vinylpyridine (0.5 mL) in THF (7 mL) were placed in a round bottom flask. Benzoyl peroxide (0.033 g, 3% mol) was added, and the mixture was heated to 70–75 °C for 5 hours while being stirred. The precipitate was collected by filtration, washed several times with THF, and finally dried at 60 °C overnight. Basic content of P4VP/AlPO<sub>4</sub>-11 nanocomposite was estimated by back-titration using NaOH. Five millilitre of HCl (0.2 N) was added to 0.05 g of this nanocomposite and stirred for 30 minutes. The catalyst was removed and washed successively with deionized water. The excess amount of HCl was titrated with NaOH (0.1 N) in the presence of phenolphthalein as an indicator. Basic sites content of catalyst with Al/P = 1.2 was 7.12 mmol/g.

### 2.4. General procedure for Knoevenagel condensation

The Knoevenagel condensation between benzaldehyde and malononitrile at room temperature was chosen as the standard reaction.

The general procedure was as follows: malononitrile (1.0 mmol) was dissolved with 5.0 mL water as solvent and P4VP/AlPO<sub>4</sub>-11 (0.12 g) was then added. Benzaldehyde (1.0 mmol) was added to the reaction mixture in a round bottom flask. The mixture was then stirred vigorously at room temperature for 10 minutes. After the completion of the reaction (monitored by TLC), using n-hexane/ethylacetate (18:2) as eluent, the mixture was cooled and filtered

by hot ethanol to separate the catalyst. The solvent was evaporated, and the resulting solids were obtained. Products were confirmed by means of <sup>1</sup>H and <sup>13</sup>C NMR spectroscopy. Another interesting aspect is the use of catalyst in solvent-free condition. Activity of this nanocomposite significantly increased when the reaction was carried out without solvent.

## 3. Results and discussion

### 3.1. Characterization of the catalysts

#### 3.1.1. XRD

Fig. 1 shows the X-ray powder diffraction patterns of AlPO<sub>4</sub>-11 crystal and poly(4-vinylpyridine)/AlPO<sub>4</sub>-11 with Al/P = 1.2 (Table 1, entry 3). The powder XRD pattern of AlPO<sub>4</sub>-11 (Fig. 1a) indicates that the crystals are of pure AEL structure [10,11]. The highly crystalline nature and the phase purity of the AlPO<sub>4</sub>-11 are evident from the intensities and absence of any spurious peaks. Fig. 1b shows the XRD pattern for P4VP/AlPO<sub>4</sub>-11 which has the same crystal structure and XRD pattern typical of AEL topology. It demonstrates that the AEL structure of AlPO<sub>4</sub>-11 was well retained after hybridization with P4VP. The

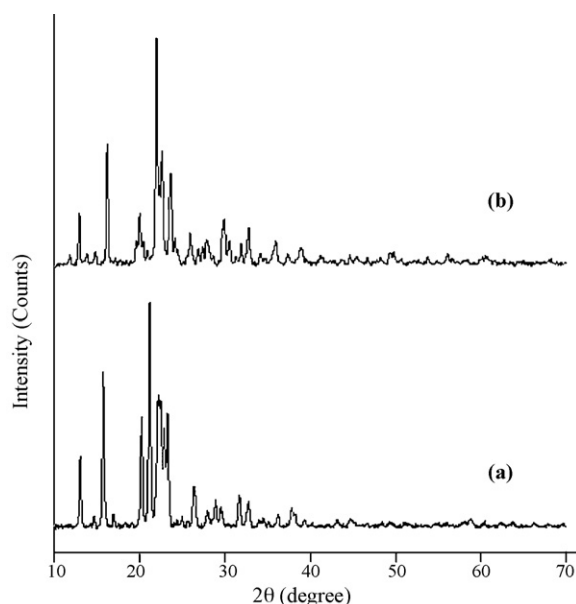


Fig. 1. XRD patterns of (a) AlPO<sub>4</sub>-11 and (b) P4VP/AlPO<sub>4</sub>-11 (Al/P = 1.2).

characteristic peaks of the  $\text{AlPO}_4$ -11 phase (i.e.  $2\theta = 13, 15, 21, 23, 26$  and  $35$ ) were observed for both patterns. Furthermore, the prominent peaks of P4VP/ $\text{AlPO}_4$ -11 sample shift to higher angles compared to microporous  $\text{AlPO}_4$ -11 due to the decrease in pore diameter.

### 3.1.2. SEM

SEM images of  $\text{AlPO}_4$ -11 (Al/P = 1.2) and P4VP/ $\text{AlPO}_4$ -11 (Al/P = 1.2) are given in Fig. 2. The surface texture of both samples show spherical aggregates of small crystals and wheat sheaf morphology [21]. No change is observed on morphology of  $\text{AlPO}_4$ -11 after hybridization with P4VP (Fig. 2c, d), which is attributed to the polymerization of 4-vinylpyridine in the pores of  $\text{AlPO}_4$ -11, which is also supported by the abrupt decrease in surface area and in pore volume as shown in Table 2.

### 3.1.3. BET

The  $\text{N}_2$  adsorption-desorption isotherm of the  $\text{AlPO}_4$ -11 (Al/P = 1.2) and P4VP/ $\text{AlPO}_4$ -11 (Al/P = 1.2) at 77 K for 7 hours was also examined (Fig. 3). The isotherm (Fig. 3a, b) exhibits a type I isotherm typical of microporous materials. The specific surface area of the samples and the pore size distributions had been calculated using Brunauer-Emmett-Teller (BET) and Barrett-Joyner-Halenda (BJH)

methods, respectively. BET surface area, total pore volume, micropore volume and micropore surface area for  $\text{AlPO}_4$ -11 and P4VP/ $\text{AlPO}_4$ -11 are presented in Table 2 (micropore volumes were determined by the  $t$ -plot method).

As can be seen from Fig. 3c, the isotherm proved the presence of varied pores with different sizes between 1–10 nm [10]. The micropore surface area and micropore volume of  $\text{AlPO}_4$ -11 is calculated about  $50.7 \text{ m}^2/\text{g}$  and  $0.28 \text{ cm}^3/\text{g}$ , respectively. We can notice that the polymerization of 4-VP into the aluminophosphate framework leads to a decrease in the surface area and micropore volume, which can be explained by a change in the pore shape due to the polymerization of 4-VP within the pores of the  $\text{AlPO}_4$ -11. The isotherm of P4VP/ $\text{AlPO}_4$ -11 (Fig. 3d) exhibits uniform distribution of pores in comparison to isotherm of  $\text{AlPO}_4$ -11 (Fig. 3c) and exhibits a smaller pore volume due to filling the pores with P4VP. It is shown that the P4VP/ $\text{AlPO}_4$ -11 nanocomposite has been successfully synthesized with a microporous form, which can act as a basic catalyst for Knoevenagel condensation.

### 3.1.4. FT-IR

The FT-IR spectra of  $\text{AlPO}_4$ -11 (Al/P = 1.2) and P4VP/ $\text{AlPO}_4$ -11 (Al/P = 1.2) are shown in Fig. 4. They have symmetric stretching bands at around  $670/\text{cm}$  and  $700/$

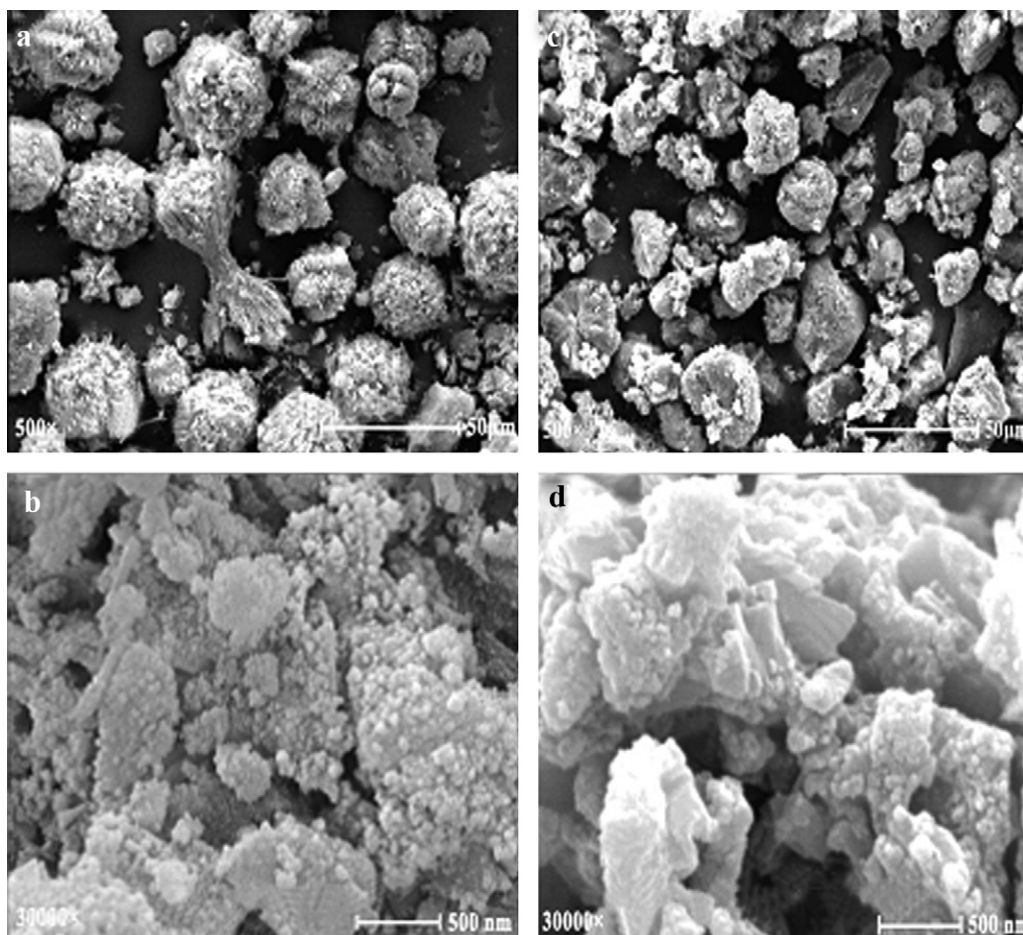


Fig. 2. Scanning electron micrographs (SEM) of (a, b)  $\text{AlPO}_4$ -11 (Al/P = 1.2) and (c, d) P4VP/ $\text{AlPO}_4$ -11 (Al/P = 1.2).



Table 2

Porosity data of  $\text{AlPO}_4$ -11 and P4VP/ $\text{AlPO}_4$ -11 samples.

Samples	BET surface area ( $\text{m}^2/\text{g}$ )	Micropore volume ( $\text{cm}^3/\text{g}$ )	Total pore Volume ( $\text{cm}^3/\text{g}$ )	Micropore surface area ( $\text{m}^2/\text{g}$ )
$\text{AlPO}_4$ -11	132.1	0.28	0.32	50.7
P4VP/ $\text{AlPO}_4$ -11	57.7	0.154	0.165	16.5

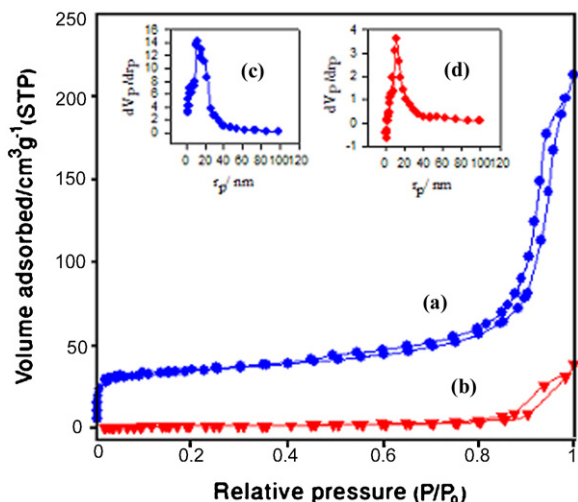


Fig. 3. The  $\text{N}_2$  adsorption-desorption isotherm of (a)  $\text{AlPO}_4$ -11 ( $\text{Al}/\text{P} = 1.2$ ) and (b) P4VP/ $\text{AlPO}_4$ -11 ( $\text{Al}/\text{P} = 1.2$ ).

cm, which correspond to the O-P-O and O-Al-O, respectively. The broad absorption band of  $\text{AlPO}_{4-n}$  molecular sieves in the range of 1000–1200/cm is due to the asymmetric stretching vibration of framework  $\text{AlO}_4^+$  and  $\text{PO}_4^-$  [22]. In addition, bands centered at around 3600, 3460 and 1619/cm can be attributed to the hydrogen-bonded hydroxyl groups and O-H vibration of  $\text{H}_2\text{O}$  [23]. The vibration bands of di-n-propylamine (DPA) in the region of 1400–1500/cm demonstrate the presence of DPA in the pores of  $\text{AlPO}_4$ -11, which remains in the pores after calcination [23]. In the FT-IR spectrum of P4VP/ $\text{AlPO}_4$ -11 (Fig. 4b), the appearance of the new bands at 1603, 1562 and 1417/cm is due to the characteristic absorptions of pyridine ring [20]. The new band at 1603/cm corresponds to the stretching vibration absorption of C-N bond and the bands at around 1562 and 1417/cm are attributed to the stretching vibration absorption of C=C bond. The appear-

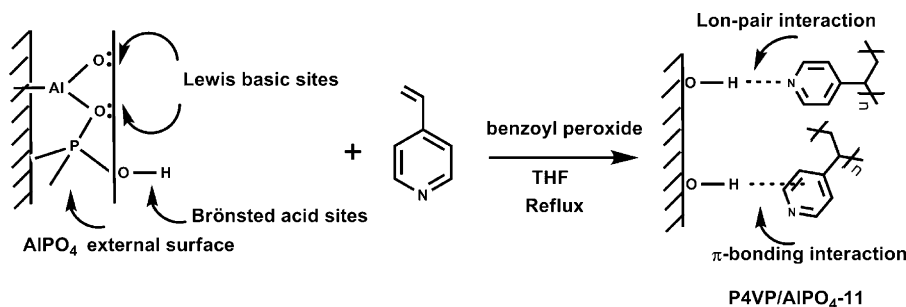
ance of the above bands indicates the successful polymerization of pyridine ring in to the  $\text{AlPO}_4$ -11 pores and the P4VP/ $\text{AlPO}_4$ -11 nanocomposite is obtained.

### 3.1.5. $\text{NH}_3$ -TPD

The TPD curve of  $\text{AlPO}_4$ -11 is shown in Fig. 5. For  $\text{AlPO}_4$ -11 with  $\text{Al}/\text{P} = 1.2$  (Table 1, entry 3), one desorption peak at 246.4 °C was assigned to ammonia desorption from weak acid sites. The result shows that most of the ammonia adsorbed on  $\text{AlPO}_4$ -11 desorbed below 400 °C. The absence of any additional peak at higher temperature indicates the absence of strong acid sites in  $\text{AlPO}_4$ -11. Yang et al. [24] proposed that the weak acid sites be derived from weak Lewis acid sites and terminal P-OH groups. The total number of the acid sites was calculated from the amount of ammonia desorbed. The amount of weak acid sites of  $\text{AlPO}_4$ -11 with  $\text{Al}/\text{P} = 1.2$  is 6.04 mmol/g.

### 3.1.6. TG-DTA

The TGA results of the  $\text{AlPO}_4$ -11 ( $\text{Al}/\text{P} = 1.2$ ), P4VP and P4VP/ $\text{AlPO}_4$ -11 ( $\text{Al}/\text{P} = 1.2$ ) under  $\text{N}_2$  atmosphere are presented in Fig. 6. The mass loss at 95 °C (around 8%, w/w) is attributed to desorption of water present in the pores and channels of the  $\text{AlPO}_4$ -11 (Fig. 6a), and there is no mass loss after this temperature, which demonstrates that the structure of  $\text{AlPO}_4$ -11 is stable after 95 °C. The weight loss of P4VP begins at 210 °C because of thermodegradation of P4VP polymer chains and the weight loss at 500 °C is around 62% (Fig. 6b). Thermo analysis of P4VP/ $\text{AlPO}_4$ -11 shows two steps of mass loss (Fig. 6c). The first step (around 5%, w/w) that occurs at 90 °C is related to desorption of water. The second step (around 5%, w/w), which appeared at 350 °C is attributed to degradation of the polymer. By comparing the P4VP and P4VP/ $\text{AlPO}_4$ -11 curves, one can find that the weight loss of P4VP/ $\text{AlPO}_4$ -11 occurs at a higher temperature; it illustrates that P4VP/ $\text{AlPO}_4$ -11 had higher thermal stability and slower degradation rate than P4VP. As a result, thermal stability of catalyst by hybridization is



Scheme 2. Schematic representation of P4VP interaction with  $\text{AlPO}_4$ -11 and preparation of P4VP/ $\text{AlPO}_4$ -11.

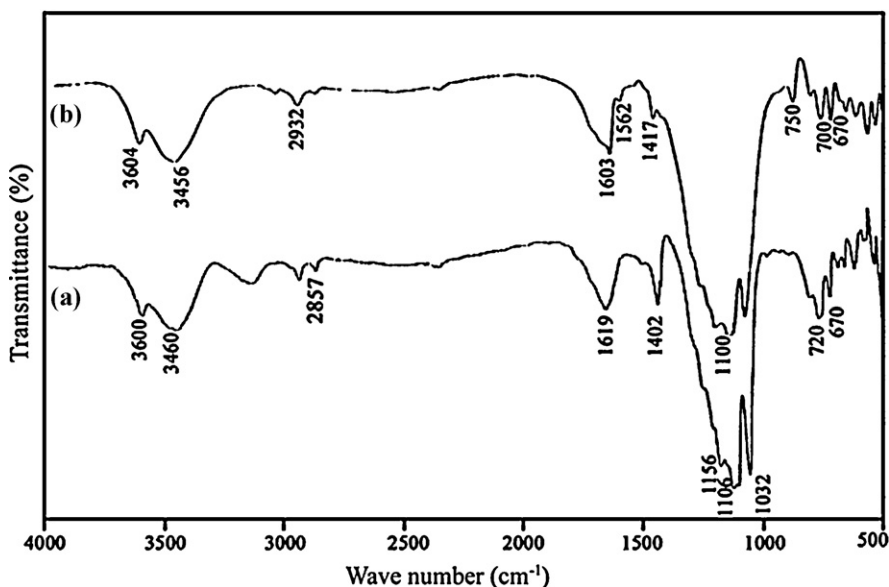


Fig. 4. FT-IR spectra of (a) microporous  $\text{AlPO}_4$ -11 (Al/P = 1.2) and (b) P4VP/ $\text{AlPO}_4$ -11 (Al/P = 1.2).

improved and it is a very remarkable point for catalytic application.

### 3.2. Catalytic activity

This novel nanocomposite was synthesized and characterized. In order to investigate the possible activity of P4VP/ $\text{AlPO}_4$ -11 in the Knoevenagel condensation (Scheme 3), we investigated AlPOs prepared with various Al/P molar ratios for choosing the best support for attachment of poly(4-vinylpyridine) on the surface of  $\text{AlPO}_4$ -11. We have chosen  $\text{AlPO}_4$  to support the P4VP because the structure of open-framework AlPOs has some specific characteristics compared to mesoporous SBA-15:

- controllable pore size distributions in  $\text{AlPO}_4$  can be achieved by using different organic amine templates in contrast to constant pore size of SBA-15 [25];
- adjusting acidic-basic property of  $\text{AlPO}_4$  surface by using various Al/P ratios for synthesis of  $\text{AlPO}_4$  to obtain a high surface area as well as a high number of surfaces –OH groups [26,27];

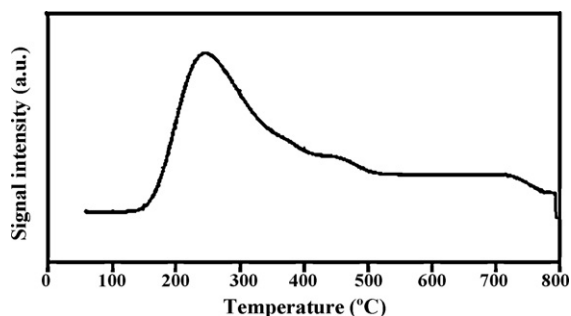


Fig. 5.  $\text{NH}_3$ -TPD curve of the  $\text{AlPO}_4$ -11.

- micropore structure of  $\text{AlPO}_4$  compared to mesopore structure of SBA-15 could help to increase shape-selectivity (described in section 3.5) [28]. The active sites of the catalyst are considered to be the pyridyl functional groups that confined located on the micropores of the  $\text{AlPO}_4$ -11. Accordingly, P4VP/ $\text{AlPO}_4$ -11 could act as a shape selective catalyst in the Knoevenagel reaction.

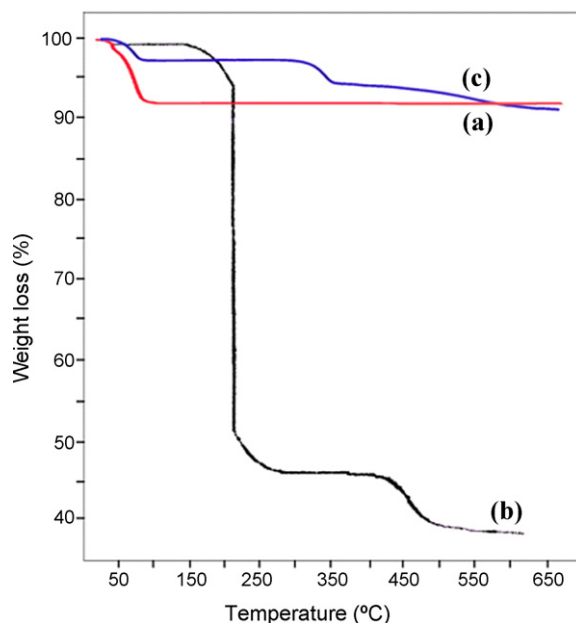
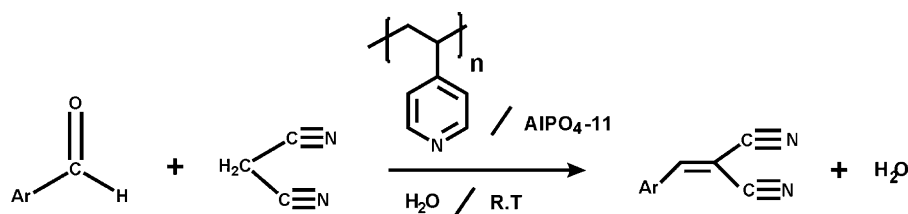


Fig. 6. TGA curves of (a) microporous  $\text{AlPO}_4$ -11 (Al/P = 1.2) (b) P4VP (c) P4VP/ $\text{AlPO}_4$ -11 (Al/P = 1.2).

Scheme 3. Knoevenagel condensation catalyzed by P4VP/AlPO<sub>4</sub>-11.

The effect of various reaction parameters on the condensation of benzaldehyde with malononitrile were studied at room temperature using P4VP/AlPO<sub>4</sub>-11 nanocomposite as catalyst and the results are as follows.

### 3.2.1. Effect of the Al/P ratio of support on the catalytic activity

Various AlPO<sub>4</sub>-11 with different Al/P molar ratios in molar gel composition have been synthesized (Table 1) and tested for Knoevenagel condensation (Table 3). According to the results in Table 3, these supports with different Al/P ratios and surface acid-base properties lead to different results in the Knoevenagel condensation. The best yield was obtained when the Al/P was 1.2 (this ratio is in accordance with the XRF result). The yield of the reaction was increased with a decrease in P molar ratio. To discuss this behavior the following concept should be mentioned:

- at first, the Brönsted acid sites strength of AlPO<sub>4</sub> increases with increasing P content due to the increase in surface OH groups (Scheme 2). After that, by further increasing the P content, the sample is changed to phosphate salt form, and it leads to a decrease in Brönsted acid sites;
- a possible adsorption mode for P4VP on the surface of AlPO<sub>4</sub> was a lone pair interaction between the pyridine nitrogen atom and the hydroxyl protons (Brönsted acid sites) on the surface of AlPO<sub>4</sub> [9]. Other interactions would be an interaction involving the pyridine ring  $\pi$ -interaction or a less specific Van Der Waals interaction between the aliphatic polymer chain backbone and the AlPO<sub>4</sub> surface [29]. Two of these possibilities were previously illustrated schematically in Scheme 2.

Table 3

Effect of the composition of the support (Al/P molar ratio) on the catalytic activity of P4VP/AlPO<sub>4</sub>-11<sup>a</sup>.

Entry	Al/P ratio	Time (min)	Yield (%) <sup>b</sup>	Basic sites (mmol/g)
1	1.0:2.5	10	80	7.10
2	1.0:1.8	10	60	6.20
3	1.1:1.73	10	60	6.80
4	1.1:1.3	10	70	7.12
5	1.1:0.9	10	98	7.12

<sup>a</sup> Reaction conditions: benzaldehyde (1 mmol), malononitrile (1 mmol), catalyst (0.12 g), H<sub>2</sub>O (5 mL), room temperature.

<sup>b</sup> Isolated yield.

According to the above concepts, it can be concluded that by increasing the amount of P in the support, the interaction of pyridine nitrogen atoms with the hydroxyl protons (Brönsted acid sites) on the surface of AlPO<sub>4</sub> increases, and the basic sites of the catalyst decreases. So, the activity of the catalyst decreases. Accordingly, we can conclude that the best support is AlPO-11 with Al/P = 1.2 molar ratio. This support has some P groups, and so hydroxyl groups that are enough to interact with P4VP for supporting them and the other free pyridine groups can act as basic sites. These results are in accordance to the data presented in Table 3 about basic content of catalysts prepared with various Al/P molar ratios. On the other hand, the nanocomposite containing the support with a high amount of P (Al/P = 1/2.5, entry 1) shows a higher catalytic activity than the supports with Al/P = 1/1.8 to 1.1/1.3 (entry 2, 3, 4). According to the concept mentioned in section (a), by further increasing the P content, the sample is changed to phosphate salt form and it leads to a decrease in Brönsted acid sites. Therefore, the interaction of pyridine nitrogen atoms with the hydroxyl protons (Brönsted acid sites) on the surface of AlPO<sub>4</sub> decreases and the basic sites of the catalyst increases (Table 3, entry 1).

### 3.2.2. Effect of solvent

The sensitivity of a heterogeneously catalyzed reaction to different solvents can usually be of extreme importance depending on the nature of the catalyst support material. The Knoevenagel condensation was carried out at room temperature using various non polar and polar solvents such as H<sub>2</sub>O, Toluene, acetonitrile, tetrahydrofuran, n-

Table 4

Effect of solvent on Knoevenagel condensation<sup>a</sup>.

Solvent	Time (min)	Yield (%) <sup>b</sup>
Water	10	98
Acetonitrile	10 160 <sup>c</sup>	5 20
Toluene	10 120 <sup>c</sup>	35 70
Tetrahydrofuran	10 120 <sup>c</sup>	– –
n-hexan	10 160 <sup>c</sup>	35 80
Solvent-free	2	98

<sup>a</sup> Reaction conditions: P4VP/AlPO<sub>4</sub>-11 (0.12 g), benzaldehyde (1 mmol), malononitrile (1 mmol), solvent (5 mL), room temperature.

<sup>b</sup> Isolated yield.

<sup>c</sup> Time of maximum yield.

hexan and solvent-free conditions (Table 4). Our investigations indicate that polar solvents, such as H<sub>2</sub>O with highest polarity, gave high yield in a shorter period of time at ambient temperature because of the polar nature of P4VP/AlPO<sub>4</sub>-11 nanocomposite. Despite the Knoevenagel condensation being a net dehydration, the reaction was surprisingly favored in aqueous medium [30]. The simplest interpretation of these results is due to the influence of the solvent on the transition state. The intermediate is better solvated by polar solvents and more stable in H<sub>2</sub>O as solvent. In addition, surprising results were obtained when we examined the same reactions under solvent-free condition over P4VP/AlPO<sub>4</sub>-11 catalyst. The reaction occurred much faster with higher yields at ambient temperature. This result is attributed to bringing the activated methylene compound in close proximity to the basic sites of the catalyst under solvent-free condition.

### 3.2.3. Effect of AlPO<sub>4</sub>-11 amount on catalytic activity of P4VP/AlPO<sub>4</sub>-11 nanocomposite

Catalytic activity of P4VP/AlPO<sub>4</sub>-11 was improved by optimizing the different amount of AlPO<sub>4</sub>-11. The results presented in Table 5 were obtained by Knoevenagel condensation over P4VP/AlPO<sub>4</sub>-11 nanocomposite prepared by different amounts of AlPO<sub>4</sub>-11 in which the amounts of the AlPO<sub>4</sub>-11 were 0.0, 0.25, 0.5 and 1 g. The best yield of Knoevenagel reaction was obtained when the ratio of AlPO<sub>4</sub>-11 (g) to 4VP (mL) was 1:1. The results presented in Table 5 reveal that the higher amount of AlPO<sub>4</sub> has no influence on the catalytic activity of the P4VP/AlPO<sub>4</sub>-11. It should be noted that the unfunctionalized AlPO<sub>4</sub>-11 is only very weakly active in the Knoevenagel condensation with less than 10% yield observed within 15 minutes. This indicated the necessity of the poly(4-vinylpyridine) coating on the pores of the AlPO<sub>4</sub>-11 to create basic sites. Also, a comparative reaction by using P4VP and P4VP/AlPO<sub>4</sub>-11 shows that P4VP/AlPO<sub>4</sub>-11 is more active and efficient because of the larger surface area and existence of micropores of P4VP/AlPO<sub>4</sub>-11 in comparison to P4VP. On the other hand, P4VP is adhesive, and this characteristic makes it hard to separate from the vessel, but after being mixed with AlPO<sub>4</sub>-11 and making P4VP/AlPO<sub>4</sub>-11 nanocomposite, it becomes powdery which is easy to be used and recycled.

### 3.2.4. Effect of catalyst amount on Knoevenagel condensation

The effect of catalyst amount on the yield of Knoevenagel condensation was investigated and the values are

Table 5

Effect of AlPO<sub>4</sub>-11 amount on catalytic activity of P4VP/AlPO<sub>4</sub>-11 nanocomposite<sup>a</sup>.

Amount of AlPO <sub>4</sub> -11/ 4-VP (g/mL)	Time (min)	Yield (%) <sup>b</sup>	Basic sites (mmol/g)
0/0.5	15	75	9.50
0.25/0.5	6	98	5.20
0.5/0	15	10	–
0.5/0.5	2	98	7.12
1/0.5	5	98	7.10

<sup>a</sup> Reaction conditions: benzaldehyde (1 mmol), malononitrile (1 mmol), catalyst (0.12 g), solvent-free, room temperature.

<sup>b</sup> Isolated yield.

Table 6

Effect of catalyst amount on Knoevenagel condensation<sup>a</sup>.

Amount of catalyst (g)	Time (min)	Yield (%) <sup>b</sup>
–	240	–
0.06	15	80
0.08	6	98
0.1	5	98
0.12	2	98
0.14	2	98

<sup>a</sup> Reaction conditions: benzaldehyde (1 mmol), malononitrile (1 mmol), solvent-free, room temperature.

<sup>b</sup> Isolated yield.

shown in Table 6. When the amount of catalyst increased from 0.08 to 0.12 g, the reaction was completed in a shorter time because of the availability of more basic sites, which favors the dispersion of more active species. With a further increase in catalyst amount to 0.14 g, it had no remarkable effect on the percentage of yield and reaction time. It is not of practical interest to use a large amount of catalyst. So, the quantity of 0.12 g has been chosen as the optimized weight of catalyst for Knoevenagel condensation. In order to test the catalytic performance in the absence of catalyst, the Knoevenagel condensation was carried out in absence of catalyst at room temperature. No reaction was observed in the absence of catalyst at room temperature, which indicates an importance of the catalytic activity of the P4VP/AlPO<sub>4</sub>-11.

### 3.3. Application of P4VP/AlPO<sub>4</sub>-11 in Knoevenagel condensation of various aldehydes with malononitrile

In order to test the versatility of the catalyst, we submitted various aromatic aldehydes and hetero-aromatic aldehydes with malononitrile in the presence of P4VP/AlPO<sub>4</sub>-11 nanocomposite at room temperature in aqueous and solvent-free conditions (Scheme 3). Selected results are shown in Table 7. All reactions investigated were almost completed in 2–90 minutes in water as solvent and 1–7 minutes in solvent-free condition. Hetero-aromatic aldehydes such as 2-pyridine carbaldehyde (entry 11, 12) provided very good yields. Aromatic aldehydes with electron withdrawing groups (–NO<sub>2</sub>, –Cl) also offered good yields and the reactions were completed in short times. Also, in the case of electron donating groups (–OCH<sub>3</sub>, –CH<sub>3</sub>), reasonably good yields were observed but demanded a little more reaction time.

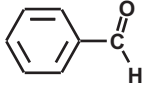
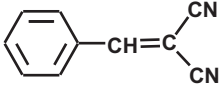
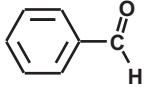
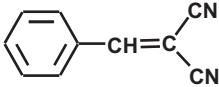
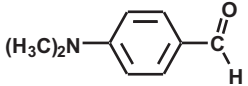
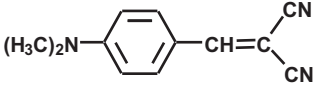
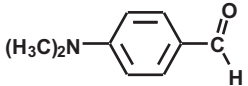
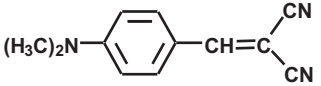
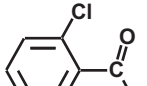
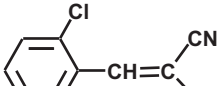
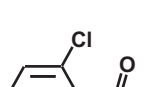
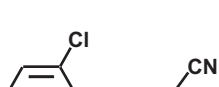
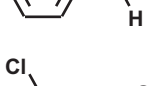

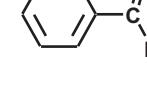
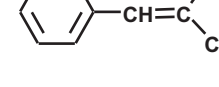
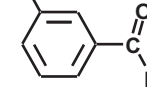
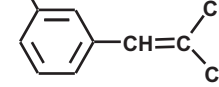
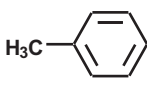
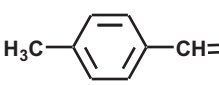
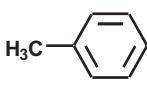
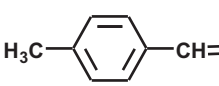
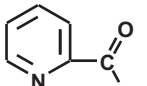
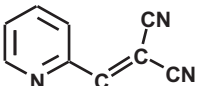
### 3.4. Reusability of the catalyst

In order to know whether the catalyst would lose catalytic activity during the Knoevenagel condensation, after completion of the reaction, the catalyst was filtered and washed thoroughly with acetone and dried in an oven at 80 °C for 4 hours to be used in the next reaction cycle. It was observed that the activity of the catalyst just decreased to 90% after performing five regeneration processes. Basic content of reused catalyst (after five cycles) was estimated by back-titration using NaOH. Basic sites content of reused catalyst (after five cycles) was 6.44 mmol/g. By comparing the amounts of basic sites

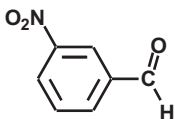
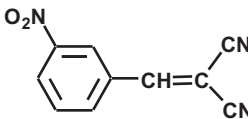
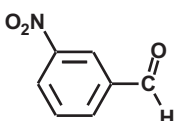
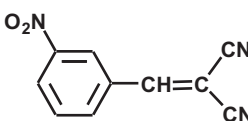
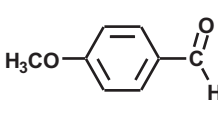
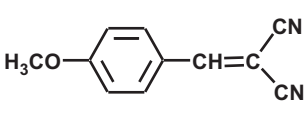
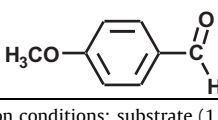
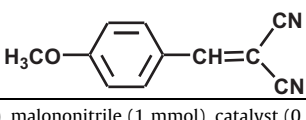


Table 7

Knoevenagel condensation of aromatic aldehydes and malononitrile catalyzed by P4VP/AlPO<sub>4</sub>-11<sup>a</sup>.

Entry	Substrate	Product	Time (min)	Yield (%) <sup>b</sup>	Mp (°C)		Ref.
					Found	Reported	
1			2	98	81–83	82–84	[31,32]
2 <sup>c</sup>			10	98	81–83	82–84	[31,32]
3			7	98	182–183	180–182	[33]
4 <sup>c</sup>			70	60	182–183	180–182	[33]
5			1	98	96–98	95–96	[34]
6 <sup>c</sup>			8	98	96–98	95–96	[34]
7			1	98	97–100	102–103	[35]
8 <sup>c</sup>			5	98	97–100	102–103	[35]
9			3	98	132–134	133–135	[36]
10 <sup>c</sup>			90	98	132–134	133–135	[36]
11			1	98	92–94	95–96	[36]
12 <sup>c</sup>			10	98	92–94	95–96	[36]

**Table 7** (Continued)

Entry	Substrate	Product	Time (min)	Yield (%) <sup>b</sup>	Mp (°C)		Ref.
					Found	Reported	
13			5	98	102–104	103–104	[37]
14 <sup>c</sup>			17	98	102–104	103–104	[37]
15			2	98	112–113	114–115	[38]
16 <sup>c</sup>			27	98	112–113	114–115	[38]

<sup>a</sup> Reaction conditions: substrate (1 mmol), malononitrile (1 mmol), catalyst (0.12 g, P4VP/AlPO<sub>4</sub>-11), solvent-free, room temperature.

<sup>b</sup> Isolated yield.

<sup>c</sup> Solvent: H<sub>2</sub>O.

(6.44 mmol/g) in the reused catalyst with the fresh catalyst (7.12 mmol/g), it can be found that the basic site content of the catalyst is reduced around 9% after performing five regeneration processes. In addition, the yield of the product is decreased to 90% (the yield was reduced around 8%). These results indicate that the activity of catalyst is reduced after performing five regeneration processes because the amount of basic sites of the catalyst is reduced. It can be related to some polymer leaching.

### 3.5. Investigation on shape selectivity of P4VP/AlPO<sub>4</sub>-11

Compared to the Knoevenagel reactions of ethyl cyanoacetate with aromatic aldehydes, the reactions of malononitrile with the same aromatic aldehydes were especially rapid and were completed in 1–2 minutes because the electron withdrawing ability of CN group is stronger than that of carbonyl or carboxylic group. In this section, we want to compare the shape selectivity of P4VP/AlPO<sub>4</sub>-11 and P4VP/SBA-15 (prepared in our previous study). Although, basic sites content of P4VP/AlPO<sub>4</sub>-11 (7.12 mmol/g) is almost similar to the P4VP/SBA-15

**Table 8**

Comparison of shape selectivity in Knoevenagel condensation over different catalysts<sup>a</sup>.

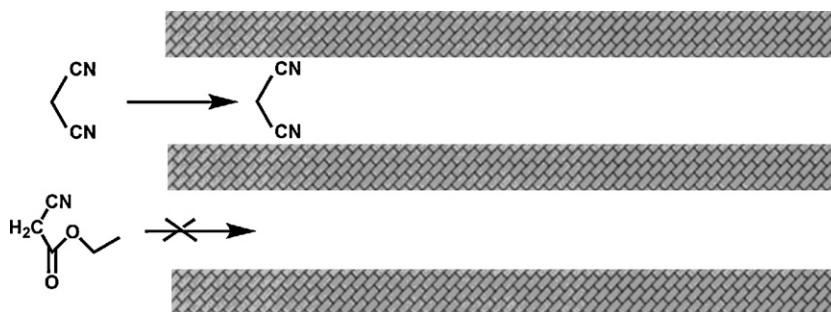
Catalyst	Time (min)	Temperature (°C)	Yield (%) <sup>b</sup>	Ref.
P4VP/SBA-15	30	40	95	Our previous study
	10 <sup>c</sup>	RT	98	
P4VP/AlPO <sub>4</sub> -11	30	40	50	This work
	120	80	90	
	10 <sup>c</sup>	RT	98	

<sup>a</sup> Reaction conditions: benzaldehyde (1 mmol), ethyl cyanoacetate (1 mmol), catalyst (0.12 g), H<sub>2</sub>O (5 mL).

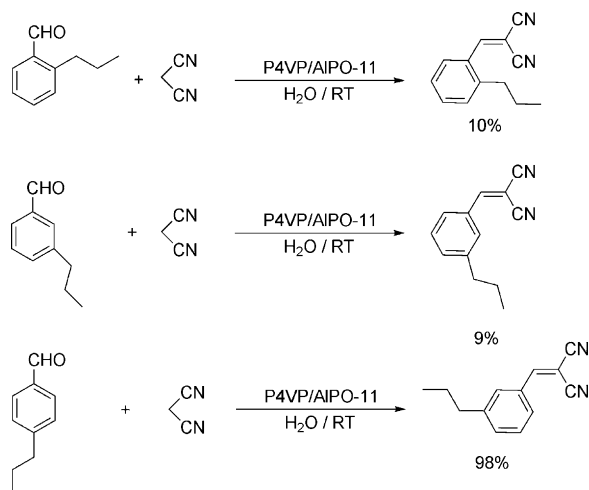
<sup>b</sup> Isolated yield.

<sup>c</sup> Reaction conditions: benzaldehyde (1 mmol), malononitrile (1 mmol), catalyst (0.12 g), H<sub>2</sub>O (5 mL).

(7.24 mmol/g), the yield of Knoevenagel condensation with ethyl cyanoacetate as an activated methylene compound as shown in Table 8, on P4VP/SBA-15 was higher than P4VP/AlPO<sub>4</sub>-11. It was demonstrated that microporous AlPO<sub>4</sub>-11 showed better shape selectivity in



**Scheme 4.** Shape-selectivity of P4VP/AlPO<sub>4</sub>-11 in Knoevenagel condensation of benzaldehyde with various active methylene compounds.



**Scheme 5.** Shape-selectivity of P4VP/AlPO<sub>4</sub>-11 in Knoevenagel condensation of bulky aldehydes with malononitrile.

comparison to mesoporous SBA-15 because the pore size of microporous AlPO<sub>4</sub>-11 is smaller than SBA-15. The ethyl cyanoacetate molecules are too large to penetrate the narrow pores of P4VP/AlPO<sub>4</sub>-11 but the malononitrile molecules are smaller than ethyl cyanoacetate molecules so they can penetrate easily into the pores of P4VP/AlPO<sub>4</sub>-11 (Scheme 4). But ethyl cyanoacetate molecules cannot penetrate the pores of P4VP/AlPO<sub>4</sub>-11, and so the condensation reaction between benzaldehyde and ethyl cyanoacetate occurs on the external surface of the catalyst. Accordingly, the activity of P4VP/AlPO<sub>4</sub>-11 for Knoevenagel condensation between benzaldehyde and ethyl cyanoacetate is low. On the other hand, this condensation in the presence of P4VP/SBA-15 with the same basic sites of catalyst occurs very easily. These results suggest that shape selectivity of AlPO<sub>4</sub>-11 for ethyl cyanoacetate compared to SBA-15 is due to the pore size of AlPO<sub>4</sub>-11 and not to the difference in basic sites content.

Also, in order to examine the shape-selectivity of the catalyst, 2-propylbenzaldehyde, 3-propylbenzaldehyde and 4-propylbenzaldehyde were allowed to react with malononitrile in the presence of P4VP/AlPO<sub>4</sub>-11 as a catalyst. As shown in Scheme 5, the catalyst was able to discriminate between the aldehydes with different steric effects. As we can see from the Scheme 5, alkene produced major only from 4-propylbenzaldehyde. From these data, we can conclude that the reaction just occurs in the micropores of the catalyst and it doesn't occur on the outer surface of the catalyst or in the solution.

#### 4. Conclusion

In conclusion, a novel organic–inorganic hybrid polymer P4VP/AlPO<sub>4</sub>-11 has been synthesized and has been applied for Knoevenagel condensation of aldehydes with malononitrile in aqueous and under solvent-free conditions, in good yield. The active sites in P4VP/AlPO<sub>4</sub> are related to pyridyl functional groups, which are confined within the surface –OH groups of the AlPO<sub>4</sub>-11. This new

heterogeneous catalyst is a practical alternative for the application of Knoevenagel reactions in view of the following advantages such as: high catalytic activity, high yield and 100% selectivity to the condensation product at room temperature, shape-selectivity, easy separation of the catalyst by simple filtration, waste minimization without any side reactions such as self condensation, dimerization or rearrangements and reusability of catalyst. Many scientists recently reported the use of mesoporous molecular sieves as catalysts in Knoevenagel condensation. However, to the best of our knowledge, there is no report on Knoevenagel reaction over microporous polymer/aluminophosphate nanocomposite. Controllable pore size distribution, adjusting acidic-basic property of AlPO<sub>4</sub> surface and shape-selectivity of AlPO<sub>4</sub> compared to SBA-15 are the main reasons for the application of AlPO<sub>4</sub>-11 as support. This new catalyst can be useful for basic heterogeneous catalysis, particularly for the shape-selective synthesis under solvent-free condition. Our results here demonstrate the feasibility of applying microporous AlPO<sub>4</sub>-11 as catalyst supports for synthesis the shape-selective heterogeneous catalysts that are comparable to SBA-15 mesoporous catalyst supports. We believe that investigating the structure of microporous aluminophosphates is useful for the catalyst design and future development of the application of these materials as support.

#### Acknowledgments

Supported by Islamic Azad University, Shahreza Branch (IAUSH) Research Council and Center of Excellence in chemistry, which is gratefully acknowledged.

#### References

- [1] L. Martins, D. Cardoso, *Quim. Nova.* 29 (2006) 358.
- [2] L. Martins, W. Hölderich, P. Hammer, D. Cardoso, *J. Catal.* 271 (2010) 220.
- [3] R.J. Davis, *J. Catal.* 216 (2003) 396.
- [4] A.P. Wight, M.E. Davis, *Chem. Rev.* 102 (2002) 3589.
- [5] K. Yamamoto, T. Tatsumi, *Chem. Mater.* 20 (2008) 972.
- [6] S.T. Wilson, B.M. Lok, C.A. Messina, T.R. Cannan, E.M. Flanigen, *J. Am. Chem. Soc.* 104 (1982) 1146.
- [7] J. Yu, R. Xu, *Acc. Chem. Res.* 36 (2003) 481.
- [8] H.O. Pastore, S. Coluccia, L. Marchese, *Annu. Rev. Mater. Res.* 35 (2005) 351.
- [9] V. Caballero, F.M. Bautista, J.M. Campelo, D. Luna, R. Luque, J.M. Marinas, A.A. Romero, I. Romero, M. Rodríguez, I. Serrano, J.M. Hidalgo, A. Llobet, *J. Mol. Catal. A: Chem.* 308 (2009) 41.
- [10] Q. Wang, G. Chen, S. Xu, *Micropor. Mesopor. Mater.* 119 (2009) 315.
- [11] G. Zhu, S. Qiu, F. Gao, G. Wu, R. Wang, B. Li, Q. Fang, Y. Li, B. Gao, X. Xu, O. Terasaki, *Micropor. Mesopor. Mater.* 50 (2001) 129.
- [12] F. Romilda, V.G. Marcus, O.P. Heloise, C. Dilson, *Micropor. Mesopor. Mater.* 53 (2002) 135.
- [13] P. Tian, Z.M. Liu, Z.B. Wu, L. Xu, Y.L. He, *Catal. Today* 93 (2004) 735.
- [14] R.J. Kalbasi, M. Kolahdoozan, M. Rezaei, *Mater. Chem. Phys.* 125 (2011) 784.
- [15] R.J. Kalbasi, M. Kolahdoozan, K. Shahabian, F. Zamani, *Catal. Commun.* 11 (2010) 1109.
- [16] M. Králik, A. Biffis, *J. Mol. Catal. A: Chem.* 177 (2001) 113.
- [17] B. Vaughan, E. Marand, *Micropor. Mesopor. Mater.* 112 (2008) 77.
- [18] B. Vaughan, J. Peter, E. Marand, M. Bleha, *J. Membr. Sci.* 316 (2008) 153.
- [19] S.M. Yang, Y.M. Wu, *Appl. Catal. A.* 192 (2000) 211.
- [20] R.J. Kalbasi, M. Kolahdoozan, A. Massah, K. Shahabian, *Bull. Korean Chem. Soc.* 31 (2010) 2618.
- [21] A.J. Holmes, S.J. Kirkby, G.A. Ozin, D. Young, *J. Phys. Chem.* 98 (1994) 4617.

- [22] F. Lili, Q. Xingyi, L. Zheng, Z. Yuelin, L. Xingguo, *Chin. J. Catal.* 30 (4) (2009) 340.
- [23] Y. Ma, N. Li, S. Xiang, *Micropor. Mesopor. Mater.* 86 (2005) 329.
- [24] X. Yang, H. Ma, Zh. Xu, Y. Xu, Zh. Tian, L. Lin, *Catal. Commun.* 8 (2007) 1232.
- [25] S.H. Jhung, H.K. Kim, J.W. Yoon, J.S. Chang, *J. Phys. Chem. B.* 110 (2006) 9371.
- [26] X. Li, W. Zhang, G. Liu, L. Jiang, X. Zhu, C. Pan, D. Jiang, A. Tang, *React. Kinet. Catal. Lett.* 79 (2003) 365.
- [27] G. Liu, Zh. Wang, M. Jia, X. Zou, X. Zhu, W. Zhang, D. Jiang, *J. Phys. Chem. B.* 110 (2006) 16953.
- [28] K. Joseph Antony Raj, E.J. Padma Malar, V.R. Vijayaraghavan, *J. Mol. Catal. A: Chem.* 243 (2006) 99.
- [29] G.K. Agarwal, J.J. Titman, M.J. Percy, S.P. Armes, *J. Phys. Chem. B.* 107 (2003) 12497.
- [30] M.J. Climent, A. Corma, I. Dominguez, S. Iborra, M.J. Sabater, G. Sastre, *J. Catal.* 246 (2007) 136.
- [31] G. Postole, B. Chowdhury, B. Karmakar, K. Pinki, J. Banerji, A. Auroux, *J. Catal.* 269 (2010) 110.
- [32] S.D. Sharma, P. Gogoi, D. Konwar, *Indian. J. Chem.* 46 (2007) 1672.
- [33] F. Santamarta, P. Verdia, E. Tojo, *Catal. Commun.* 9 (2008) 1779.
- [34] C. Yue, A. Mao, Y. Wei, M. Lu, *Catal. Commun.* 9 (2008) 1571.
- [35] M. Hosseini-Sarvari, H. Sharghi, S. Etemad, *Chin. J. Chem.* 25 (2007) 1563.
- [36] B.M. Reddy, M.K. Patil, K.N. Rao, G.K. Reddy, *J. Mol. Catal. A: Chem.* 258 (2006) 302.
- [37] M. Gupta, R. Gupta, M. Anand, *Beilstein. J. Org. Chem.* 5 (2009) 1.
- [38] M.B. Gawande, R.V. Jayaram, *Catal. Commun.* 7 (2006) 931.